A SIMPLIFIED OXIDATION MODEL FOR DEFECTIVE NUCLEAR FUEL

K. Shaheen
Supervisor: B.J. Lewis
Department of Chemistry and Chemical Engineering, Royal Military College of Canada,
PO Box 17000, Kingston, Ontario, Canada

Abstract

The rare occurrence of sheath defects may lead to contact between the fuel and coolant, which may lead to fuel hyperstoichiometry, thus degrading fuel thermal performance and raising the potential for centreline melting. By simplifying a published mechanistic model, a semi-empirical model has been developed to predict fuel hyperstoichiometry using a one-dimensional oxygen transport equation coupled to a two-dimensional temperature equation, improving numerical robustness for possible implementation into fuel performance codes. The model has been validated against experimental measurements from commercial defective elements for normal operation, and has been used to predict the response of defective fuel under accident conditions.

1 Introduction

In a CANDU (CANada Deuterium Uranium) reactor, sintered UO_2 pellets are stacked within a Zircaloy sheath to form a fuel element, with helium gas in the fuel-to-sheath gap. In rare cases (less than 0.1 % in CANDU reactors), defects can develop in the fuel sheath, possibly for one of the following reasons[1,2]: fretting, delayed hydrogen cracking, stress corrosion cracking, or fuel fabrication flaws. The degraded thermal performance of defective fuel increases the possibility of fuel centreline melting. The CNSC (Canadian Nuclear Safety Commission), which regulates the operation of civilian nuclear technology in Canada, prohibits the presence of molten fuel in safety analyses. Thus, there is a need to better understand defective fuel behaviour[3].

2 Review of Defective Fuel Research & Project Goals

Upon the introduction of a defect to the Zircaloy sheath, the following processes can take place in the defective fuel element:

- Gap transport: D_2/D_2O gas that enters the defect flows along the axial direction in the fuel-to-sheath gap, causing oxidation and hydriding of the Zircaloy sheath.
- Crack transport: D_2/D_2O gas flows principally in the radial direction in the fuel cracks, which can result in fuel oxidation at the pellet surface of the fuel cracks.

- Oxygen transport: Excess oxygen liberated in the fuel oxidation reaction diffuses in the solid fuel matrix due to concentration and thermal gradients in the solid UO_{2+x}.
- Heat transfer: An increased fuel hyperstoichiometry may result in a decrease in the fuel thermal conductivity and thus lead to an increased fuel temperature.

To address all of these phenomena, a fully mechanistic treatment for defective fuel oxidation was developed by Higgs[4] and validated against experimental data for fuel hyperstoichiometry. A representation of the azimuthally-symmetric, two-dimensional mechanistic model, including key equations, is shown in Figure 1.

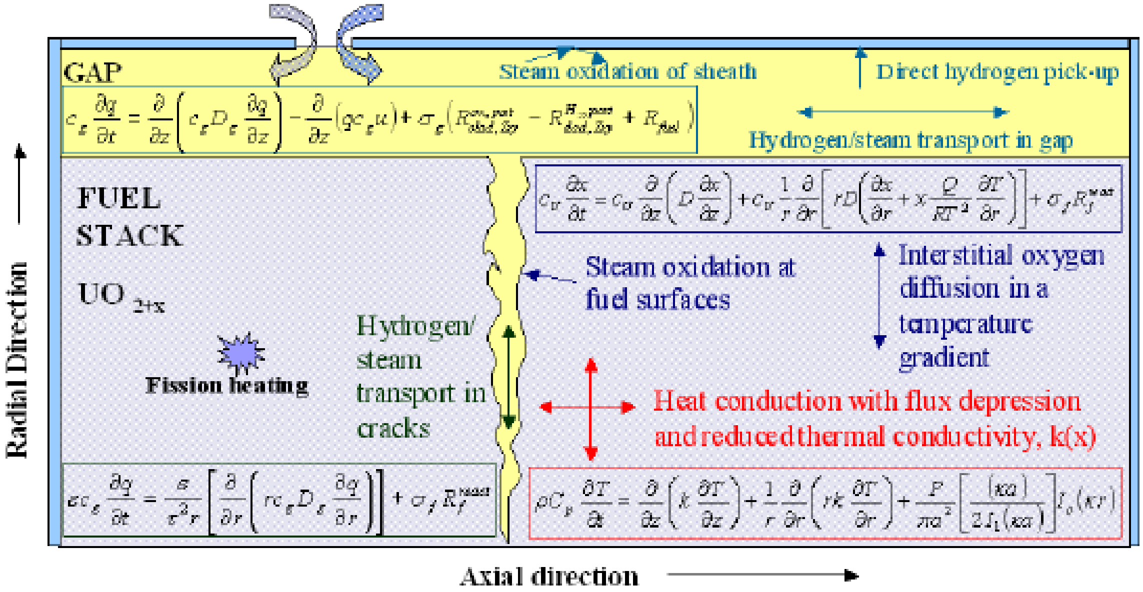

Figure 1 Geometric representation of the mechanistic model for defective fuel. Taken from [4].

The sophisticated mechanistic model, which uses four coupled, time-dependent partial differential equations (PDEs) to simulate defective fuel, is numerically intensive and thus difficult to solve. For increased robustness and ease of implementation into available fuel performance codes, the model needs to be numerically simplified, while using empirical correlations where possible to include important phenomena, particularly hydrogen/steam gas-phase transport (and the resultant atmospheric oxygen potential in the fuel-to-sheath gap and fuel cracks). Accordingly, the goal of the current work is to increase the numerical robustness of the model by developing a reduced set of coupled equations, while capturing underlying phenomena and producing agreement with available experimental data for fuel hyperstoichiometry.

3 Model Development

3.1 Thermodynamics of the Uranium-Oxygen System

The uranium-oxygen phase diagram is shown in Figure 2 below[5].

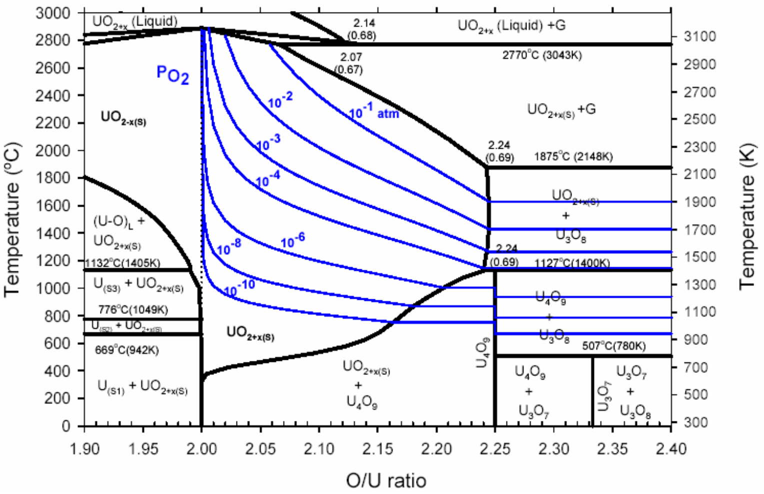

Figure 2 Uranium-oxygen phase diagram showing oxygen partial pressure in equilibrium with temperature and O/U ratio. Taken from [5].

At any given temperature, the equilibrium stoichiometry deviation, x_e, relates to the extent of stoichiometry deviation at which the oxygen partial pressure within the fuel is equal to the partial pressure in the surrounding atmosphere (indicated by the partial pressure lines in Figure 2). The equilibrium partial pressure is associated with the reaction:

$$2D_2O(g) \Leftrightarrow O_2(g) + 2D_2(g) \qquad \textbf{Equation 1}$$

The oxygen partial pressure is related to the D_2/D_2O ratio through the equilibrium constant for the above reaction, which is given by:

$$K = \frac{p_{D_2}^2 p_{O_2}}{p_{D_2O}^2} \qquad \textbf{Equation 2}$$

Accordingly, the equilibrium stoichiometry deviation can be related to the D_2/D_2O ratio. Since there is negligible difference in expressing the reaction equilibrium with respect to the D_2/D_2O or H_2/H_2O ratio[5], an expression for x_e is developed as a function of the H_2/H_2O ratio.

3.2 Model Concept and Cornerstone Equations

Based on the observed results of mechanistic model simulations, the maximum stoichiometry deviation occurs under the defect site, where H_2/H_2O ratio in the fuel-to-sheath gap is lowest. It is postulated that the area in the fuel element under the sheath defect constitutes an 'engine' for the hyperstoichiometry throughout the element. While some oxidation is expected to occur in areas not located under the defect, the relative increase in the H_2/H_2O ratio in these regions would suppress the reaction. Therefore, the axial stoichiometry deviation profile in the fuel element can be attributed to solid-state transport of oxygen from the primary oxidation site as a result of the oxygen concentration gradient (which can be treated as a first-order rate process). A semi-empirical model can thus be conceptualized as shown in Figure 3 below:

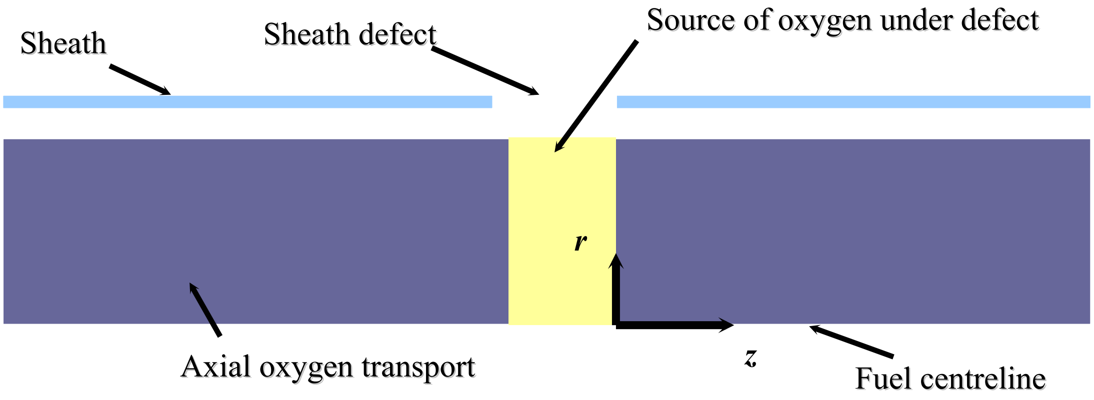

Figure 3 Concept diagram for the semi-empirical model.

Since the oxidation reaction is only modelled under the defect site, a one-dimensional adaptation of the oxygen transport equation in the mechanistic model can be considered:

$$c_u \frac{\partial x}{\partial t} = c_u \frac{1}{r}\frac{\partial}{\partial r}\left[rD\left(\frac{\partial x}{\partial r} + x\frac{Q^*}{RT^2}\frac{\partial T}{\partial r} \right)\right] + \sigma_{fuel} R_{fuel}^{react} \qquad \textbf{Equation 3}$$

where x is the stoichiometry deviation in the fuel, t (s) is time, r (m) is radial position, and T (K) is the fuel temperature. The diffusion coefficient is represented by D, and the term $rDx\frac{Q^*}{RT^2}\frac{\partial T}{\partial r}$ represents the diffusive oxygen flux along a thermal gradient, a mechanism referred to as the Soret effect, wherein the term Q^* refers to the molar effective heat of transport. The fuel surface-area-to-volume ratio is represented by σ_{fuel}. The fuel oxidation/reduction reaction term, R_{fuel}^{react}, can be described as:

$$R_{fuel}^{ox} = c_u \alpha \sqrt{(1-q)p_t}\,(x_e - x), \quad \text{for } x < x_e \qquad \textbf{Equation 4}$$

$$R_{fuel}^{red} = c_u \alpha \sqrt{qp_t}\,(x_e - x), \quad \text{for } x > x_e \qquad \textbf{Equation 5}$$

where R_{fuel}^{ox} and R_{fuel}^{red} represent oxidation and reduction processes of the fuel, respectively. The parameter c_u is the molar density of UO_2. The parameter q represents the H_2 mole fraction, p_t is the total system pressure, and α is the temperature-dependent surface-exchange coefficient.

The change in stoichiometry deviation with respect to axial separation from the defect site z_{sep} can be represented by a first-order kinetic process:

$$\frac{dx}{dz_{sep}} = -\xi x \qquad \textbf{Equation 6}$$

where ξ is a relaxation length dependent on the fuel and defect conditions.

Together, Equation 3 and Equation 6 provide a two-dimensional representation of oxygen diffusion to describe the stoichiometry deviation x in the oxidized UO_{2+x} fuel for the defective element. A two-dimensional representation for heat conduction in the fuel pellets to determine the temperature profile is:

$$c_u C_p \frac{\partial T}{\partial t} = \frac{\partial}{\partial z}\left(k\frac{\partial T}{\partial z} + \frac{1}{r}\frac{\partial}{\partial r}\left(rk\frac{\partial T}{\partial r}\right) + \frac{P_{lin}}{\pi a_p^2}\left[\frac{(\kappa a_p)}{2I_1(\kappa a_p)}\right] I_o(\kappa r)\right) \qquad \textbf{Equation 7}$$

Here, C_p is the specific heat capacity expressed as a function of stoichiometry deviation and temperature and k is the stoichiometry-dependent fuel thermal conductivity. The term $\frac{P_{lin}}{\pi a_p^2}\left[\frac{\kappa a_p}{2I_1(\kappa a_p)}\right] I_0(\kappa r)$ represents the heat generation in the fuel due to fission, accounting for the effects of flux depression in the fuel pellet. In this heat source term, P_{lin} is the variable linear power rating of the fuel element, a_p is the radius of the fuel pellet, and κ is the inverse neutron diffusion length.

3.3 Development of Empirical Correlations

Correlations are needed to determine the values of q and ξ in order to solve Equations 3 and 6 for the stoichiometry deviation. A sensitivity analysis of the stoichiometry deviation, as predicted by the mechanistic model with respect to different fuel conditions, was performed, and it was determined that the correlations should be functions of linear power rating, defect geometry (number of defects, defect sizes, and distances between defects), and Post-Defect Residence Time (PDRT). These parameters were varied within the following ranges:

Table 1 Variable parameters used to develop empirical correlations

Parameter	Range (Units)	Units
Linear power rating	20 → 65	kW m^{-1}
Number of defects	1 → 4	N/A
Defect size (axial length)	0.1 → 80	mm
Distance between defects	0 → 450	mm
Post-Defect Residence Time (PDRT)	1 → 760	d

A typical simulation of a defective fuel element operating at 40 kW m^{-1} for 380 d, with a single 5-mm defect at the element midplane, is shown in Figure 4 using the mechanistic model of Higgs. Similar simulations were used to benchmark the empirical correlations.

Assuming a constant axial relaxation length ξ with respect to axial separation from the defect site z_{sep}, Equation 6 can be solved to give:

$$\xi = -\frac{1}{z_{sep}} \ln\left(\frac{x(z_{sep})}{x_{def}}\right) \qquad \textbf{Equation 8}$$

By running the mechanistic model for the full range of element linear power ratings and distances between defects, a full space of values for ξ was produced for both single- and double-defect cases. The curve-fitting software TableCurve3D™ was then used to reproduce these values. The resulting correlations are used to predict the axial oxidation profile away from the defect site(s).

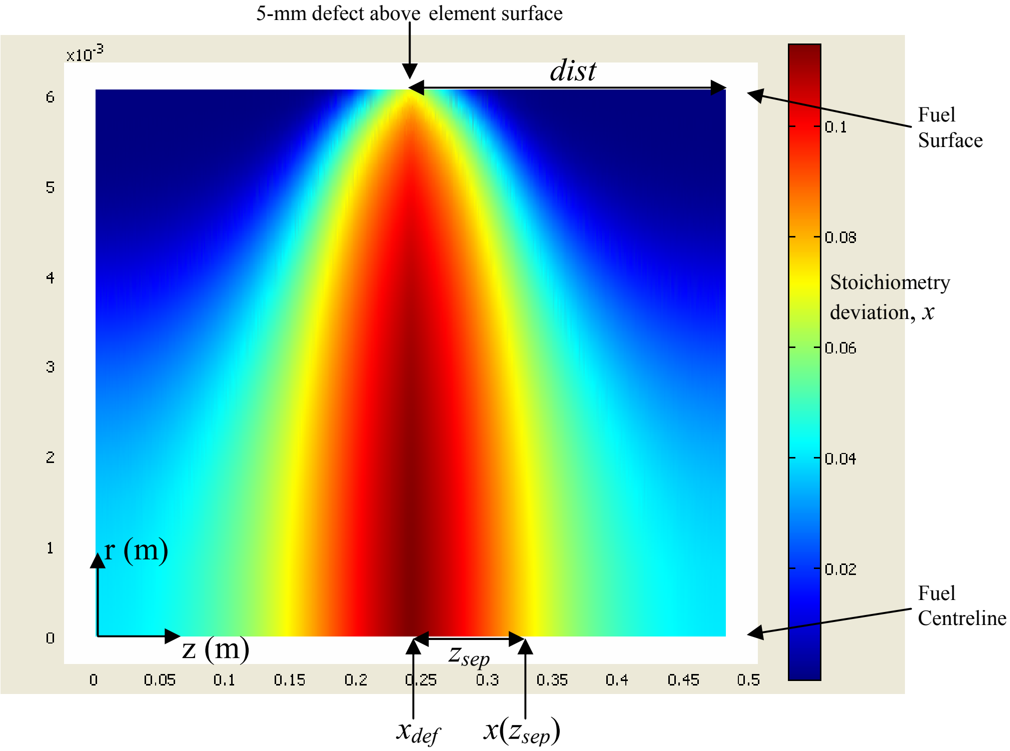

Figure 4 Sample stoichiometry deviation results from the mechanistic model for a fuel element of length 0.482 m and radius 6.075 mm operating at 40 kW m^{-1} for 380 days with a 5-mm defect at the element midplane.

Under the defect site, the H_2 mole fraction, q, is required in order to simulate the oxidation reaction. For the simulation shown in Figure 4, the time-dependent value of q under the defect site at the fuel centreline is shown in Figure 5.

In the semi-empirical model, the time-dependence of q is implicitly captured by assuming an appropriate constant value for the full element PDRT. For the range of element linear power ratings and defect sizes given in Table 1, the minimum and time-dependent average values of q, referred to as q_{min} and q_{ave} respectively, were found (it should be noted that, in finding the minimum value of q, the brief initial period where q increases from near-zero to a maximum is not considered since the values in this period represent a numerical artifact of the initial condition assumed for the mechanistic model). These values were reproduced using orthogonal Legendre Polynomials, which can be defined recursively to the required precision (due to the model's sensitivity to q) without sacrificing accuracy.

™ Tablecurve3D is a trademark of SPSS, Inc.

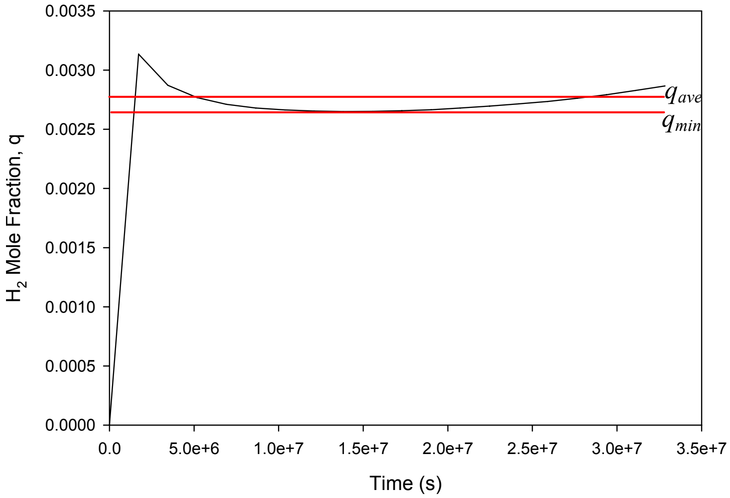

Figure 5 Centreline *q* beneath the site of a 5-mm defect for a fuel element operating at 40 kW m^{-1} for a PDRT of 380 d with the end-of-life, average, and local minimum values shown.

Given the centreline value of *q*, the radial profile produced by the mechanistic model can be approximated using a linear profile as shown in Figure 6.

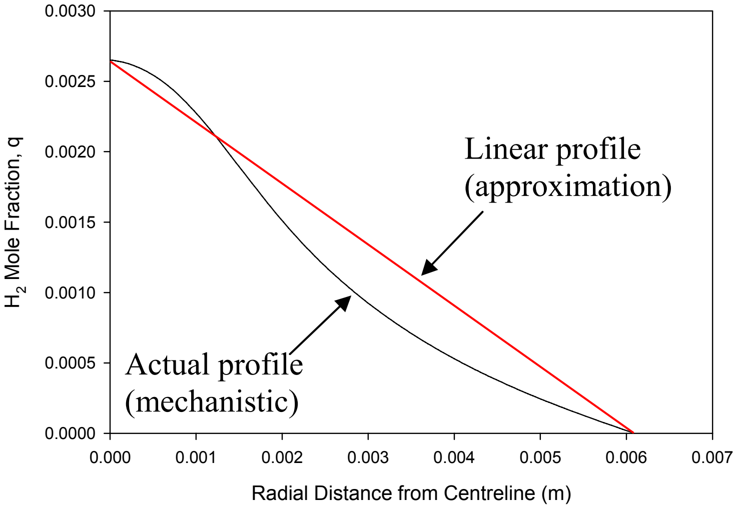

Figure 6 Radial profile of *q* under a 5-mm defect for a fuel element operating at 40 kW m^{-1} at t = 100 d, with the linear approximation shown in red.

By introducing the correlations for H_2 mole fraction and axial relaxation length to the equations outlined is Section 3.2, the fuel oxidation state and temperature can be predicted by solving a system of two PDEs.

The various constants, parameters and empirical correlations for the simplified fuel oxidation models are detailed in Ref. 6.

3.4 Numerical Implementation

The semi-empirical model was implemented in the COMSOL Multiphysics™ platform installed on Windows XP Professional®. A sample geometry representing the fuel in COMSOL is shown in Figure 7.

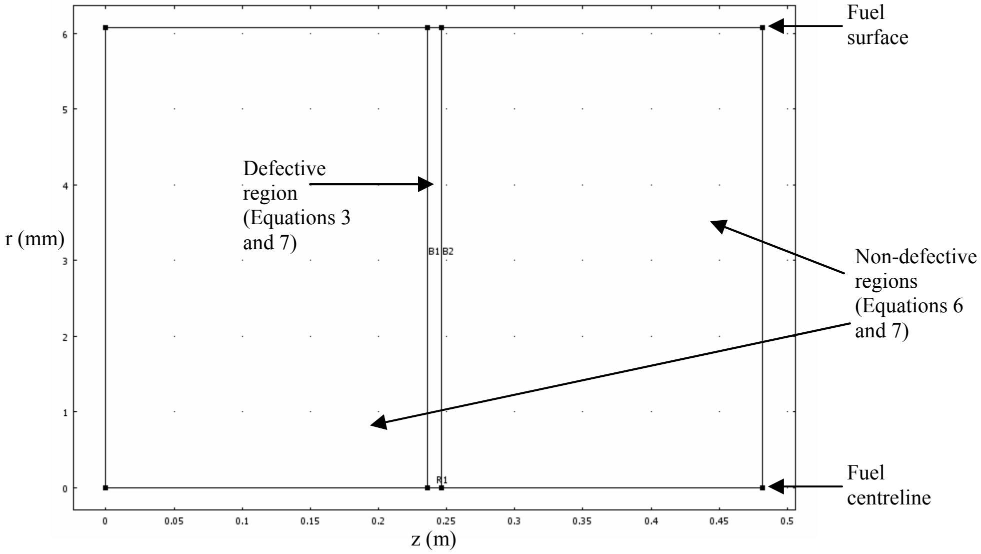

Figure 7 Sample representation of the geometry of a fuel element with a single 10-mm defect.

The one-dimensional oxygen transport equation (Equation 3) is solved assuming no oxidation at initialization, an axial symmetry condition at the centreline, and no reaction ($x = x_e$) at the fuel surface. The temperature equation (Equation 7) is solved assuming an initial temperature equal to the fuel surface temperature, which is evaluated according to the methodology of Lewis et. al.[7], and insular boundaries at the axial edges and centreline of the element.

4 Results and Discussion

4.1 Model Validation and Observed Limitations

The semi-empirical fuel oxidation model was used to predict the oxidation and temperature profiles of 10 commercial defective fuel elements, which were measured for their O/M ratios. In particular, the results were compared to the predictions of the mechanistic model and to experimental data provided by Atomic Energy of Canada Limited (AECL) at the Chalk River Laboratories (CRL)[8]. At the CRL, the oxygen-to-metal (O/M) ratio was measured for each of the defective elements using a coulometric titration (CT) technique. For a representative case, a comparison of results is shown in

---

™ COMSOL Multiphysics is a trademark of Comsol AB.

® Windows XP Professional is a registered trademark of Microsoft Corporation.

Figure 8. The conservative semi-empirical model uses the correlations for q_{min}, while the best-estimate model uses the correlations for q_{ave}, as outlined in Section 3.3.

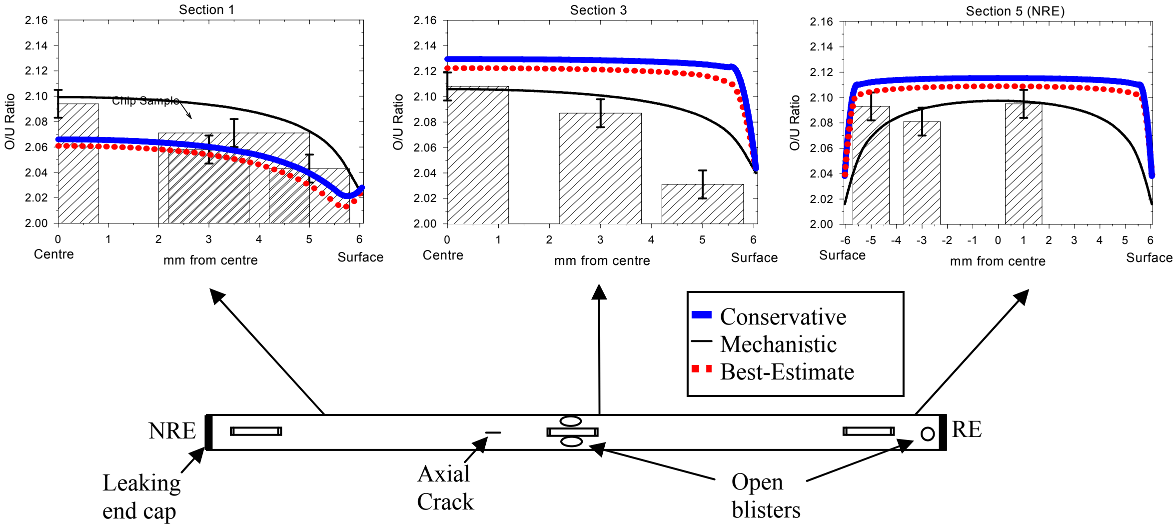

Figure 8 Representative comparison of model predictions to CRL measurements of O/U ratio.

There were no in-reactor measurements of the fuel centreline temperature, and so only the temperature values from the semi-empirical and mechanistic models can be compared. In general, the predicted results of the O/M ratio compare well with the mechanistic model predictions, as well as to the measured CT data. Also, the predictions of the centreline temperature typically vary by less than ~100 K (up to 216 K), suggesting reasonable agreement between the two models. Fuel centreline melting is never predicted for these ten commercial defective cases.

While the semi-empirical prediction is generally conservative compared to the mechanistic prediction, in some cases there is a slight underprediction of the fuel stoichiometry deviation and fuel centreline temperature, highlighting some limitations of the model. Most significantly, by reducing the oxygen transport equation to one dimension, conservation of oxygen mass is no longer maintained in the non-defective regions of the fuel. Simulations have been performed demonstrating that using a two-dimensional oxygen transport equation re-introduces conservation of mass and eliminates the underprediction of fuel hyperstoichometry. However, the use of a two-dimensional equation would increase the complexity of the model, which runs contrary to the goals of this work, and so this approach was not adopted.

4.2 Application to Transient Analysis

One of the benefits of a semi-empirical treatment for fuel oxidation is the increased robustness and simplicity of the model, which make the treatment easier to implement in a fuel code to determine the performance of defective fuel elements. Specifically, it is necessary to know if and when the fuel undergoes centreline melting. It has been demonstrated in this work that, for typical normal operating conditions (NOC), fuel melting is not expected. However, a remaining question is whether centreline melting could occur in a previously defective element (where the fuel has already been oxidized) during an accident scenario, such as a Loss-of-Coolant Accident (LOCA).

During a LOCA, as a result of coolant voiding and the positive void coefficient, there is a sharp increase in the power rating of a fuel bundle, and a concurrent temperature increase in the fuel sheath and fuel itself for a short duration. The increased fuel temperatures are depicted in Figure 9 based on a BEAU (Best Estimate And Uncertainty) methodology performed by NSS (Nuclear Safety Solutions) for a safety analysis[9].

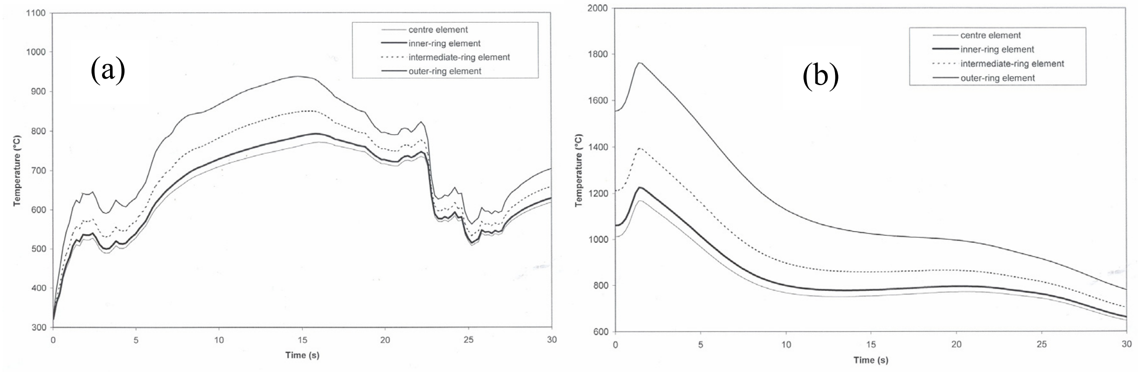

Figure 9 Transients for typical BEAU conditions for (a) fuel sheath temperature and (b) fuel centerline temperature. Taken from [9].

The mechanistic and semi-empirical models were used to simulate a fuel element undergoing a LOCA for 3 s under the conditions for normalized power (assuming an initial linear power rating of 63 kW m^{-1}) and sheath temperature given by the BEAU analysis. Three possible scenarios were considered assuming (i) an intact element, (ii) a defective element with no fuel-to-sheath gap, (iii) a defective element with a fuel-to-sheath gap with an estimated 10-μm thickness. A comparison of predicted fuel centreline temperatures for these three scenarios, and for the mechanistic and semi-empirical models, is shown in Figure 10.

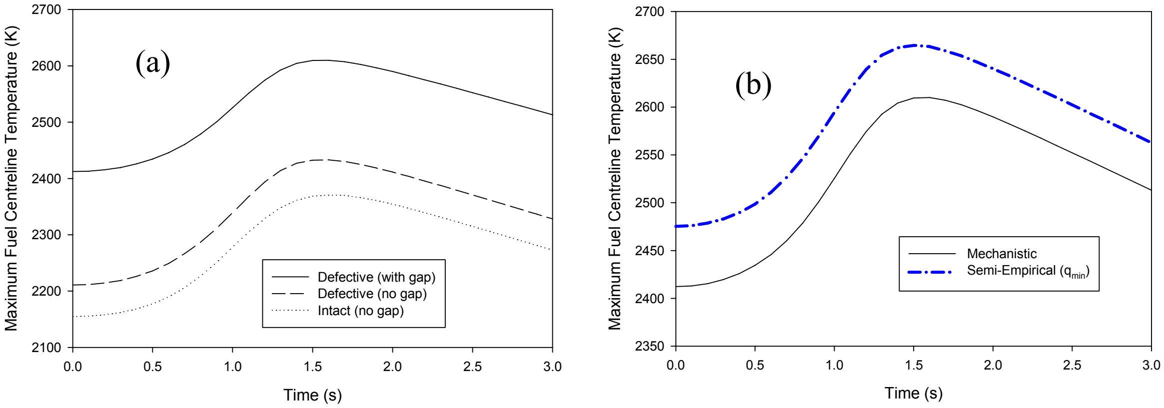

Figure 10 Predicted fuel centreline temperature history for the power pulse using (a) the mechanistic model for intact and defective fuel simulations and (b) the mechanistic and semi-empirical models for defective fuel (with a gap).

The temperatures reached during the LOCA are beneath the incipient melting temperature for UO_2. However, it is also of interest to determine whether the fuel stoichiometry changes during the power pulse. Simulations were therefore performed with the mechanistic model where the radial profile of the fuel stoichiometry deviation was examined under the defect site at various times (see Figure 11(a)) for the given fuel centerline temperature history in Figure 10. As expected, the oxidation state remains unchanged, which indicates that there is insufficient time during the power pulse for the fuel oxidation reaction kinetics and solid-state diffusion of interstitial oxygen to occur.

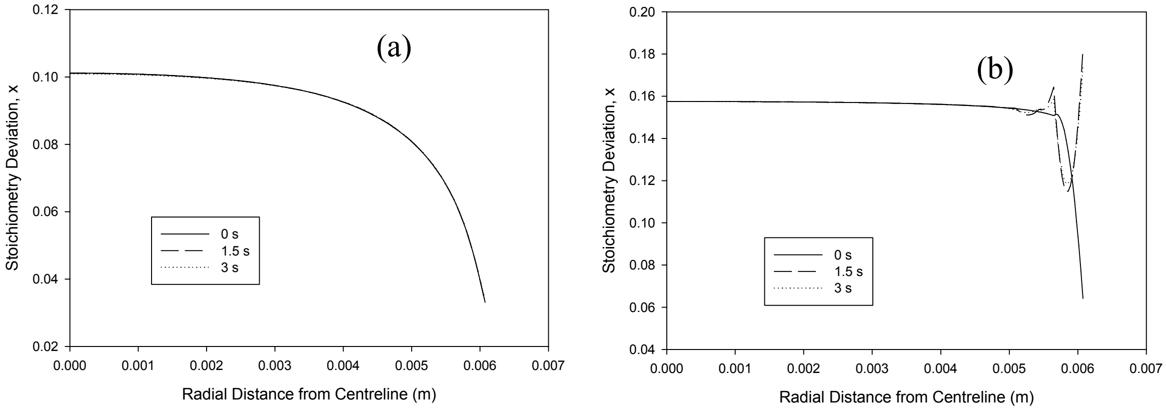

Figure 11 (a) Mechanistic model and (b) semi-empirical (q_{min}) model predictions of the radial profile of the fuel stoichiometry deviation under the defect site at several times from the start of the transient.

The same simulation was also performed with the semi-empirical model (Figure 11(b)). A similar result is obtained although there is a little fluctuation in the stoichiometry deviation curve at and near the fuel surface position. This fluctuation arises as a numerical artifact of the surface boundary condition (where x is set equal to x_e) in contrast to the use of a zero-flux condition for the mechanistic model. Nevertheless, this slight effect does not affect the radial profile away from the fuel surface.

In fact, with any possible metal-water reaction, an increased concentration of hydrogen could potentially lower the oxygen potential, thus decreasing the likelihood of fuel oxidation. Moreover, with the presence of hydrogen, the fuel reduction kinetics are considerably faster than that for fuel oxidation as observed in high-temperature annealing experiments conducted at the University of California (UCL)-Berkeley[10]. Thus, one would not expect further fuel oxidation during the transient.

5 Conclusions and Recommendations

A robust semi-empirical model has been developed for predicting the oxidation behaviour of typical defective CANDU fuel elements. As desired, the current model is generally conservative or in agreement with published experimental data for fuel stoichiometry deviation, and with the mechanistic model for fuel stoichiometry deviation and temperature. The semi-empirical model has been tested for both normal and typical transient circumstances (involving a typical power pulse due to a loss-of-coolant accident). As demonstrated, there is no centreline melting and in particular, no change in the oxidation state of the fuel during the power pulse starting from a high power rating. The semi-empirical model could potentially be incorporated into fuel performance codes[11,12] in order to include the effects of fuel oxidation on fuel performance behaviour with possible failure of the sheath during normal and reactor accident conditions.

References

1. A.M. Manzer, “Survey of Post-Defect Behaviour of CANDU Fuel,” AECL Report CRNL-2395, September 1982.
2. B.J. Lewis, W.T. Thompson, F. Akbari and C. Thurgood, “A Fuel Oxidation Model for Operating Defective Fuel Elements,” COG Report 02-2122, April 2003.
3. A. Viktorov and M. Couture, “Regulatory Activities in the Area of Fuel Safety and Performance,” Canadian Nuclear Safety Commission, Presented at the 9th Int. Conf. On CANDU Fuel, Belleville, ON, 17-21 September 2005.
4. J. Higgs, “Modelling Oxidation Behaviour in Operating Defective Nuclear Reactor Fuel Elements,” PhD. Thesis, Royal Military College of Canada, January 2006.
5. J.D. Higgs, B.J. Lewis, W.T. Thompson and Z. He, “A conceptual model for the fuel oxidation of defective fuel,” J. Nucl. Mater. 366 (2007) 99-128.
6. K. Shaheen, “A Semi-Empirical Oxidation Model for Defective Nuclear Fuel,” Royal Military College, MASc Thesis, December 2007.
7. B.J. Lewis, W.T. Thompson, J. Higgs, F. Akbari and C. Thurgood, “Modelling of Fuel Oxidation Behaviour in Operating Defective Fuel Elements,” CANDU Owners Group Report COG 03-2098, March 2004.
8. R.A. Verrall, Z. He, J.F. Mouris, “Characterization of fuel oxidation in rods with clad-holes,” J. Nucl. Mater. 344 (2005) 240-245.
9. H.E. Sills, “Darlington NGS Phenomena Identification and Ranking Table for a Critical Break Large LOCA,” Nuclear Safety Solutions report CG037/RP/001, March 30, 2006.
10. J. Abrefah, A. de Aguiar Braid, W. Wang, Y. Khalil and D.R. Olander, “High Temperature Oxidation of UO_2 in Steam-Hydrogen Mixtures,” J. Nucl. Mater. 208 (1994) 220-245.
11. G.G. Chassie, K-S. Sim, B. Wong, G. Papayiannis, “ELESTRES Code Upgrades,” AECL, 9th International CNS Conference on CANDU Fuel, 2005.
12. A.F. Williams, “The ELOCA Fuel Modelling Code: Past, Present and Future,” 9th International CNS Conference on CANDU Fuel, 2005.